REVIEW PAPERS

W. Yan, N. Li*, Bingqiang, H*

An Investigation on Slag Resistance of Castable Refractories Containing Porous Spinel Aggregates

THE AUTHOR

The **main author, Wen Yan**, PhD, is a lecturer of Wuhan University of Science and Technology and is also doing research work on refractories and Ceramics at the Hubei Province Key Laboratory of Refractories and Ceramics (both P.R. China). His fields of research include porous ceramic, insulating refractories, reactions between molten slag and refractories.

ABSTRACT

Corrosion of three spinel based castables containing the same matrix and different porous spinel aggregates by converter slag (C/S = 3) was conducted using the static crucible test through the counting pixels method, SEM, EDAX, FACTSage thermodynamic modeling, and so on. It was found that the corrosion resistance depends on the dissolution rate of porous aggregate into slag, and the penetration resistance depends on the pore size of porous aggregates, the new phases formed from refractories and slag, and the viscosity of penetrated slag. The lowest dissolution rate of porous MgO-rich spinel aggregate into slag resulted in the best corrosion resistance of castable containing this aggregate. The least pore size of porous Al_2O_3-rich spinel aggregate, the formation of $CaO \cdot 2Al_2O_3$ and $CaO \cdot 6Al_2O_3$ from refractories and slag, and the highest viscosity of penetrated slag were responsible for the highest penetration resistance of castable containing this aggregate.

KEYWORDS

porous spinel aggregate, castable refractories, slag, penetration, corrosion

Refractories Manual 2009

1 Introduction

Traditionally dense alumina-magnesia castable refractories have been widely used as working linings due to its excellent properties and easy installation [1–7, 9–17]. The high thermal conductivity of these refractories makes the decreasing of temperature of molten steel in the ladles and the increasing of the temperature of steel shell of ladles, which result in the deformation of ladle. The temperature drop of ladle lining causes adherence of slag and steel. Thus ladles become heavier; ladles' volume decrease and the casting of steel become difficult. Some researches paid attentions to insulating of ladles, e.g. Chen et al. obtained a low density castable for steel ladle by using low density alumina-spinel aggregates, in reduced material consumption and decreased temperature on the ladle shells [6]; Sinntaro et al. introduced hollow alumina particles into the castables to decrease the density and the thermal capacity of the materials [6].

The slag resistance has a critical effect on the campaign life of alumina-magnesia refractories. Many researches have been done on the slag resistance of these refractories [1–17]. The penetration resistance depends on the microstructure of refractories and the viscosity of slag which may be changed during penetration [7–10]. We have found the slag resistance of castables containing porous corundum-spinel aggregate could be improved obviously through densificating the matrix by increasing microsilica content [7]. Mukai et al. had investigated slag penetration into MgO refractories with different porosity and pore size, and found the rate of slag penetration increased with increasing pore radius and apparent porosity of the refractory [8]. Diaz et al. found that CaO, FeO and MnO in slag could be captured by alumina and spinel in the matrix of high alumina castables, making the slag SiO_2 rich and more viscous, thus inhibiting its further penetration [9]. Oguchi and Mori found that in alumina spinel castables, CaO reacted with alumina to form CA_2 and CA_6, while MnO, FeO and Fe_2O_3 were believed to be absorbed into the spinel to form a solid solution, and then the slag becomes silica-rich and viscous, and slag penetration was limited [10].

At the same time, the corrosion resistances of the refractories also were improved by reaction between the slag and refractories [11–17]. Sarpoolaky et al. found that the reaction of the penetrating slag with the fine alumina and calcium aluminates forms a CaO-rich local liquid, which can react with corundum grain to form calcium hexaluminate layer and hercynitic spinel layer to hinder slag corrosion [11]. Sarpoolaky and Cho et al. investigated the corrosion of dense spinel by slag and found layers were formed between slag and spinel, and the layers depressed slag corrosion by dissolving dense spinel indirectly into slag [12–13]. Some experimental results show that slag corrosion resistance of castable is improved further if the spinel is rich in alumina or spinel is in situ formed during service [14–17].

Usually in the refractories the aggregates have higher corrosion and penetration resistance than matrixes. Actually, it is enough that the aggregates have the slag resistance similar to matrix [7]. We investigated the corrosion and penetration resistance of porous spinel with small pore size and found that the composition and pore size gave effects on corrosion and penetration resistance of porous spinel [18–20]. It is possible to improve the penetration and corrosion resistance by reducing pore size and controlling composition and microstructure of refractories. If the porous aggregates have suitable slag resistance, they may be used instead of dense aggregates in refractories to reduce consumption of raw materials and

* Prof. Nan Li and Prof. Bingqiang Han are at the Hubei Province Key Laboratory of Refractories and Ceramics, Wuhan University of Science and Technology. Wuhan, P.R. of China

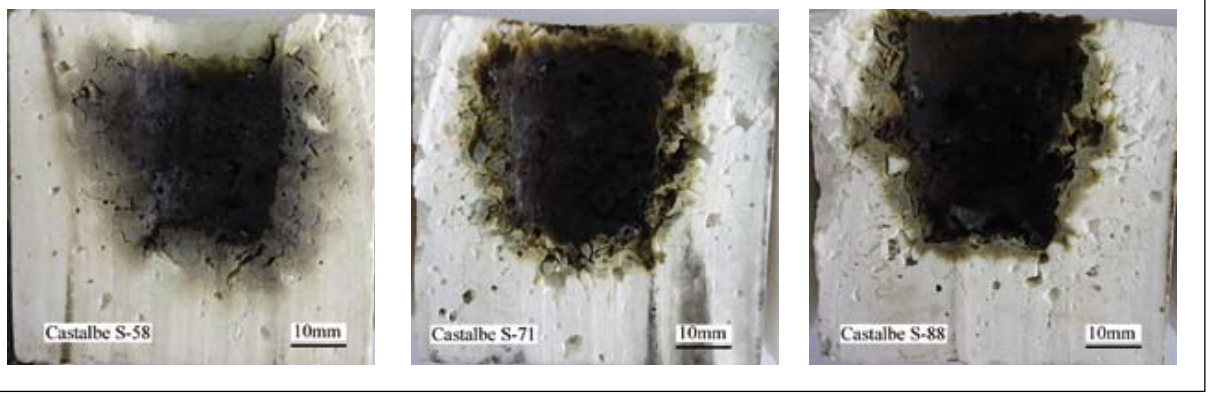

Fig. 1 • Crucibles after slag testing (vertical cut)

energy. At the same time, thermal conductivity of refractories with porous aggregates is less than that with dense aggregates, which is beneficial to furnaces insulation.

In order to study the possibility of using the lightweight aggregate in castables, we studied the influence of three porous spinel aggregates with different composition, porosity and pore size on the slag resistance of the castables.

2 Experimental

Three castables were prepared with different porous spinel aggregates but with the same matrix. The chemical compositions of matrix and slag were listed in Table 1. The composition and properties of three porous aggregates marked as S-58, S-71 and S-88 are given in Table 2. Particle size distribution of aggregates, aggregate content (65 vol-%), matrix content (35 vol-%), and water content (13.5 vol-%) were kept unchanged for all batches of castables. Three castables were named as castable S-58, castable S-71 and castable S-88 according to their different aggregates. Cubic blocks with 30 mm diameter and 40 mm deep holes were vibrocast for the crucible corrosion tests. They were cured 24 h at room temperature before drying at 110 °C for a further 24 h. The dried samples were preheated at 1100 °C for 3 h. The preheated samples filled with 30 g slag were heated at 1600 °C for 3 h in an electric chamber furnace and then furnace-cooled to room temperature.

After corrosion testing, crucibles were cross-sectioned perpendicularly to the slag-refractory interface, as shown in Fig.1. The actual corroded and penetrated areas in each sample were measured by counting pixels method. Corrosion here is defined as regions of refractory completely replaced by slag. The corrosion index Ic and penetration index Ip are obtained by following equation: $I_{C(P)} = S_{C(P)} / S_O \times 100$ %; S_O is the original section area of the crucible inner chamber; S_C is the section area of refractory completely replaced by slag; S_P is the penetrated section area.

Phase analysis was carried out by a X-ray diffractometer (Philips Xpert TMP) with a scanning speed of 2 ° / min. Bulk density and apparent porosity were measured by Archimedes' Principle with water as medium. Average pore size distribution was measured by the mercury porosimetry measurement (AutoPore IV 9500, Micromeritics Instrument Corporation). Morphology and pore structures of these specimens were observed by a scanning electron microscopy (Philips XL30). The content of SiO_2, CaO, and Fe_2O_3 in a small square with a width of 2.5 mm and a length of 3.7 mm were obtained by calibration with EDAX ZAF quantification (standardless). In order to study the changes of SiO_2, CaO, and Fe_2O_3 content, which express the depth of the penetration of slag, the contents of SiO_2, CaO, and Fe_2O_3 in six squares from the hot face to inside of this wall of crucible were measured. The distribution of six squares is shown in Fig. 2. The viscosities of penetrated slag at every square of the castables are calculated from model Riboud [21] based on the glass phase composition obtained by EDAX, and every viscosity value of slag penetrated is the average of ten values.

Table 1 • Chemical compositions of matrix and slag in mass-%

	Al_2O_3	MgO	SiO_2	CaO	MnO	Fe_2O_3
Matrix	79.21	15.62	1.51	3.37	–	0.12
Slag	2.45	7.95	14.48	45.78	2.46	26.47

3 Results and discussion

Figure 3 shows corrosion and penetration indexes of three castables after corrosion test. Castable S-58 has the highest corrosion resistance but the lowest penetration resistance, while castable S-88 has the highest penetration resistance but the lowest corrosion penetration.

Figures 4–6 show SiO_2, CaO and Fe_2O_3 contents in different squares in castables S-58, S-71 and S-88 respectively. It is found that from hot face to inside the penetration layer can be divided into three parts. No. 1 part is the square 1 and 2, in which one oxide content is very high. For castable S-58 it is Fe_2O_3, but for castables S-71 and S-88 it is CaO. No. 2 part is the square 3 and 4. In this part

Table 2 • Chemical compositions, mineral phases, average pore size, bulk density and apparent porosity of porous spinel aggregates

No.	Chemical composition / mass-%					Average pore size / μm	Bulk density / g/cm³	Apparent porosity / %	Mineral phases
	Al_2O_3	MgO	SiO_2	CaO	TFe				
S-58	57.63	39.66	0.69	0.32	0.16	8.21	2.23	37.7	Spinel, Periclase
S-71	71.12	27.47	0.42	0.24	0.13	8.13	1.95	46.6	Spinel
S-88	87.66	11.30	0.35	0.12	0.09	3.58	2.33	36.0	Spinel, Corundum

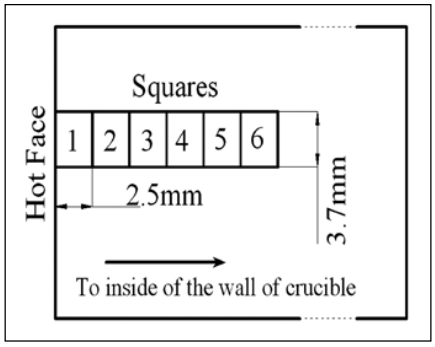

Fig. 2 • Schematic diagram of six squares' distribution

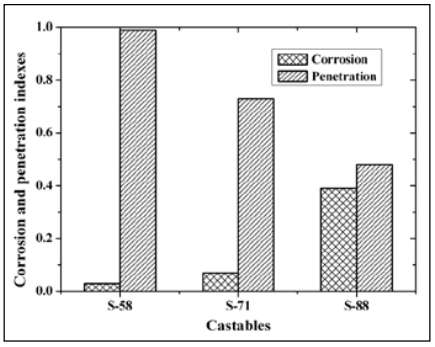

Fig. 3 • Corrosion and penetration indexes of castables

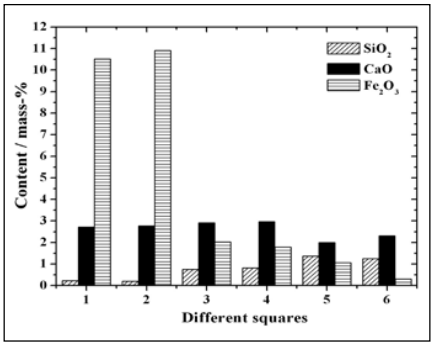

Fig. 4 • SiO_2, CaO and Fe_2O_3 contents in different squares in castable S-58

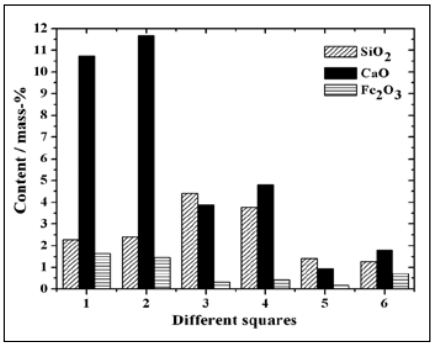

Fig. 5 • SiO_2, CaO and Fe_2O_3 contents in different squares in castable S-71

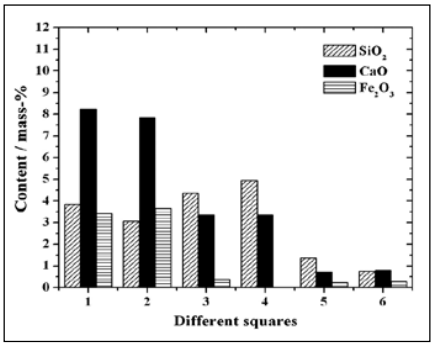

Fig. 6 • SiO_2, CaO and Fe_2O_3 contents in different squares in castable S-88

Fe_2O_3 in castable S-58 and CaO in castables S-71 and S-88 are much less than those in No. 1 part. At the same time, SiO_2 contents in No. 2 part are more than that in No. 1 part for three castables, Fe_2O_3 contents in No. 2 part is less than that in No. 1 part for castables S-72 and S-88. However CaO contents in No.2 part are slightly more than that in No. 2 part for castable S-58. No. 3 part is the square 5 and 6. In this part the contents of Fe_2O_3, SiO_2 and CaO are low, but those in castable S-58 are higher than those in castable S-72 and S-88. It also proves the difference of penetration resistance of three castables shown in Figure 3.

Figure 7 shows typical microstructure by SEM in No. 1 part of three castables. It can be seen that more (Mg, Fe)O and MgO(Al, Fe)$_2O_3$ solid solution are formed in No. 1 part of castable S-58 because of MgO better trapping Fe oxide, and more CaO are consumed to form CaO·2Al_2O_3 and CaO·6Al_2O_3 in No. 1 parts of castable S-71 and S-88. That is why castable S-58 has high Fe_2O_3 content and castables S-71 and S-88 have high CaO contents in No. 1 parts. With further penetration of molten slag, MgO and spinel in castable S-58 consumed large amount of Fe_2O_3, and Al_2O_3 in castables S-71 and S-88 consumed most of CaO, so Fe_2O_3 of castable S-58 and CaO of castables S-71 and S-88 in No. 2 parts are much less than those in No. 1 parts. Additionally, spinel in castables S-71 and S-88 also consumed Fe_2O_3, leading to Fe_2O_3 content in No. 2 parts less than that in No. 1 parts. Simultaneously, CaO in slag almost doesn't react with aggregate S-58, so CaO contents in No. 2 part are slightly more than that in No. 2 part for castable S-58. For three castables, SiO_2 in slag reacts little with refractories which can be seen in Fig. 7, so SiO_2 content in No. 2 part increases due to decrease of Fe_2O_3 and CaO contents.

The different contents of SiO_2, CaO and Fe_2O_3 in the parts of three castables, indicating the compositions of penetrated slag, affect strongly the viscosities of penetrated slag. Figure 8 shows the viscosity of penetrated slag in No. 1–2 parts of three castables calculated from model Riboud [21] based on the results of EDS analysis. It is found that the viscosity of penetrated slag in castables S-58 is much less than that in castables S-71 and S-88, and the viscosity of penetrated slag in castable S-71 is less than that in castable S-88.

The slag penetration resistance depends on the microstructure, chemical composition of castables and the viscosity of penetrated slag. Firstly, the less the porosity and the pore size, the higher the penetration resistance is. Secondly, free Al_2O_3 in castables react with CaO from slag to form CaO·2Al_2O_3 and CaO·6Al_2O_3, which fill the micropores due to the volume expansion. Thirdly, the penetration depth decreases with increase of viscosity of penetrated slag. The pore sizes of aggregates S-71 and S-58 are the similar,

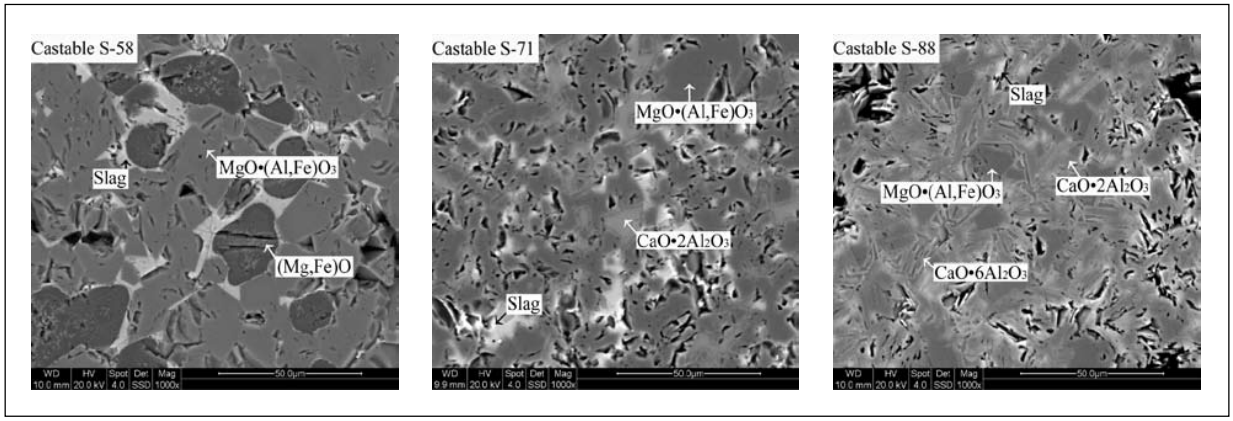

Fig. 7 • Typical microstructures by SEM in No. 1 parts of three castables

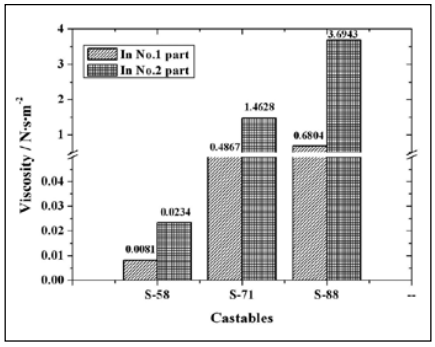

Fig. 8 • Viscosity of penetrated slag in every part of three castables calculated from model Riboud [21]

although the porosity of aggregate S-71 is bigger than that of aggregate S-58, the formation of $CaO{\cdot}2Al_2O_3$ and $CaO{\cdot}6Al_2O_3$ fills the micropores and inhibits the slag penetration, so the penetration resistance of castable S-71 is better than that of Castable S-58. In castable S-58, the pore size is the largest, the viscosity of penetrated slag is the lowest, and thus this castables has the lowest penetration resistance. In castable S-88, the pore size is the least, the viscosity of penetrated slag is the highest and the formation of $CaO{\cdot}2Al_2O_3$ and $CaO{\cdot}6Al_2O_3$ fills the micropores, so this castable has the highest penetration resistance.

The slag corrosion resistance depends on the dissolution rate of castables into slag which can be explained through thermodynamic calculation conducted with the FACT package [12]. Figure 9 shows the relation between the weight of the predicated species and alpha value at 1600 °C. For alpha = 2, the calculations were carried out with 100 g castable and 200 g slag. With increase of alpha the weight of spinel and alumina in castable S-88 decreases and abruptly drops to zero at alpha of 0.2 and 0.7, respectively. In castable S-58 with increase of alpha the spinel weight decreases and abruptly drops to zero at alpha value of 0.7, but the weight of magnesia does not change with increase of alpha. In castable S-71 the spinel weight abruptly drops to zero at alpha value of 0.9, this value is bigger than castable S-58, but it does not have magnesia which is not dissolved into slag. It means that the difference of corrosion resistance of three castables results from different chemical composition of castables. Castable S-58 has the highest corrosion resistance because its magnesia is difficult to dissolve into slag, but castable S-88 has the lowest corrosion resistance because its alumina is very easy to dissolve into slag. Castable S-71 has the corrosion resistance less than castable S-58 but higher than castable S-88 because it has neither magnesia nor alumina.

4 Conclusions

Microstructure and composition of porous spinel aggregates affect strongly the corrosion and penetration resistance of the castables. The lowest dissolution rate of porous MgO-rich spinel aggregate into slag resulted in the best corrosion resistance of castable containing this aggregate. The least pore size of porous Al_2O_3-rich spinel aggregate, the formation of $CaO{\cdot}2Al_2O_3$ and $CaO{\cdot}6Al_2O_3$ from refractories and slag, and the highest viscosity of penetrated slag were responsible for the highest penetration resistance of castable containing this aggregate.

Acknowledgements

We wish to express our thanks to the Puyang Refractories Co., Ltd for financially supporting this work.

References

[1] **Yilmaz, S.**: Corrosion of high alumina spinel castables by steel ladle slag. Ironmak. Steelmak **33** (2006) 151–156
[2] **Korgul, P., Wilson, D.R., Lee, W.E.**: Microstructural analysis of corroded alumina-spinel castable refractories. J. Europ. Ceram. Soc. **17** (1997) 77–84
[3] **Sarpoolaky, H., Zhang, S., Argent, B.B., Lee, W.E.**: Influence of grain phase on slag corrosion of low-cement castable refractories. J. Amer. Ceram. Soc. **84** (2001) 426–434
[4] **Ko, Y.**: Influence of the characteristics of spinel on the slag resistance of Al_2O_3-MgO and Al_2O_3-spinel castables. J. Amer. Ceram. Soc. **83** (2000) 2333–2335
[5] **Ko, Y.**: Role of spinel composition in the slag resistance of Al_2O_3-spinel and Al_2O_3-MgO castables. Ceram. Internat. **28** (2002) 805–810
[6] **Chen, R., He, P., Wang, N., Mon, J., Gan, F.**: Development of a Low-Density Castable for Steel Ladle. UNITECR'03 Proceedings, 2003, p. 19–23
[7] **Yan, W., Li, N., Han, B.**: Influence of microsilica content on the slag resistance of castables containing porous corundum-spinel aggregates. Internat. J. Appl. Ceram. Technol. **5** (2008) 633–640
[8] **Mukai, K., Tao, Z., Goto, K., Li, Z., Takashima, T.**: In-situ observation of slag penetration into MgO refractory. Scand. J. Metall. **31** (2002) 68–78
[9] **D'az, L.A., Torrecillas, T., Aza, A.H., Pena, P.**: Effect of spinel content on slag attack resistance of high alumina refractory castable. J. Europ. Ceram. Soc. **27** (2007) 4623–4631
[10] **Oguchi, Y., Mori, J.**: Wear mechanism of castable for steel ladle. Taikabustu Overseas **13** (1996) 43–49
[11] **Sarpoolaky, H., Zhang, S., Argent, B.B., Lee, W.E.**: Influence of grain phase on slag corrosion of low-cement castable refractories. J. Amer. Ceram. Soc. **84** (2001) 426–434
[12] **Sarpoolaky, H., Zhang, S., Lee, W.E.**: Corrosion of high alumina and near stoichiometric spinels in iron-containing silicate slags. J. Europ. Ceram. Soc. **23** (2003) 293–300
[13] **Cho, M.K., Hong, G.G., Lee, S.K.**: Corrosion of spinel clinker by CaO-Al_2O_3-SiO_2 ladle slag. J. Europ. Ceram. Soc. **22** (2002) 1783–1790
[14] **Mori, J., Onove, M., Toritani, Y., Tanaka, S.**: Structure change of alumina castable by addition of magnesia or spinel. Taikabutsu Overseas **15** (1995) 20–23
[15] **Nagai, B., Matsumoto, O., Isobe, T.**: Development of high-alumina castable for steel ladles (findings on spinel formation in alumina-magnesite castable). Taikabutsu Overseas **10** (1990) 23–28
[16] **Nanba, M., Kaneshige, T., Hamazaki, Y., Nishio, H., Ebizawa, I.**: Thermal Characteristics of Castables for Teeming Ladle. Taikabutsu Overseas **16** (1996) 17–21
[17] **Ma, X., Wang, Z., He, Q., Xu, Y.**: Development and application of Al_2O_3-MgO castable for large ladles in concasting system. China's Refract. **7** (1998) 25–29
[18] **Yan, W., Li, N.**: Effects of pore size distribution and composition on slag resistance of porous spinel. Proceedings of the Fifth International Symposium on Refractories (2007) 215–219
[19] **Wen, Y., Nan, L., Han, B.**: High-strength, lightweight spinel refractories. Amer. Ceram. Soc. Bull. **84** (2005) 9201–9203
[20] **Li, S., Li, N., Li, Y.**: Processing and Microstructure Characterization of Porous Corundum-Spinel Ceramics Prepared by in-situ Decomposition Pore Forming Technique. Ceram. Internat. **34** (2007) 1241–1246
[21] **Mills, K.C., Keene, B.J.**: Physical properties of BOS slags. Internat. Mater. Rev. **32** (1987) 1–12

Received: 15.05.2009

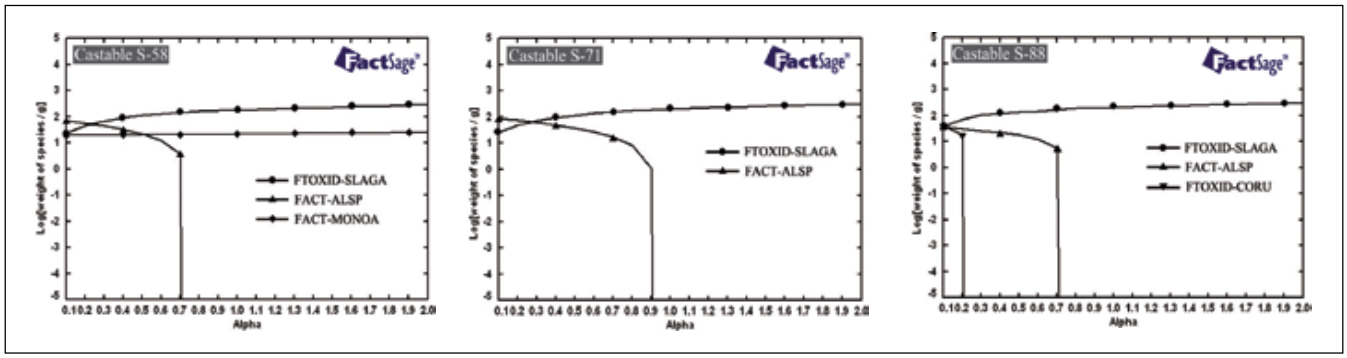

Fig. 9 • Relationship between the weight of the predicated species and alpha value FTOXID-SLAGA allowed solution of MgO, FeO, MnO, SiO_2, CaO, Al_2O_3 and Fe_2O_3. FACT-ALSP was used for spinel solutions ($MgAl_2O_4$, $MnAl_2O_4$ and $FeAl_2O_4$), which allows solution of FeO and MnO. FACT-MONOA was used for magnesia, which allows solution of FeO and MnO. FTOXID-CORU was used for alumina, which allows solution of FeO and MnO